

Experimental Determination of the Helium $2^3P_1-1^1S_0$ Transition Rate

R. G. Dall, K. G. H. Baldwin,* L. J. Byron, and A. G. Truscott

*ARC Centre of Excellence for Quantum-Atom Optics and Research School of Physical Sciences and Engineering,
The Australian National University, Canberra, ACT 0200, Australia*

(Received 12 September 2007; published 15 January 2008; corrected 17 January 2008)

We present the first experimental determination of the $2^3P_1-1^1S_0$ transition rate in helium and compare this measurement with theoretical quantum-electrodynamic predictions. The experiment exploits the very long (~ 1 minute) confinement times obtained for atoms magneto-optically trapped in an apparatus used to create a Bose-Einstein condensate of metastable (2^3S_1) helium. The $2^3P_1-1^1S_0$ transition rate is measured directly from the decay rate of the cold atomic cloud following 1083 nm laser excitation from the 2^3S_1 to the 2^3P_1 state, and from accurate knowledge of the 2^3P_1 population. The value obtained is $177 \pm 8 \text{ s}^{-1}$, which agrees very well with theoretical predictions, and has an accuracy that compares favorably with measurements for the same transition in heliumlike ions higher in the isoelectronic sequence.

DOI: 10.1103/PhysRevLett.100.023001

PACS numbers: 32.70.Cs, 12.20.Fv, 37.10.Gh, 42.50.Xa

Quantum electrodynamics (QED) is one of the most rigorously tested fundamental theories of modern physics, for which the atomic energy levels of helium and helium-like ions represent an important test bed. Helium is the simplest multielectron atom, enabling theoretical calculations to be performed with greater accuracy than for more complex species. From a theoretical standpoint, the energy levels of helium can be determined via a power series expansion of the fine-structure constant to a high level of accuracy [1] which has been tested by modern experimental advances in precision measurement. The ground-state energy has been determined using precision pulsed laser techniques to better than one part in 10^8 to derive the ground-state Lamb shift [2,3], while ultra-narrow-band cw lasers and optical frequency combs have enabled measurement of excited-state transitions with an accuracy that exceeds one part in 10^{11} , challenging Lamb shift [4] and fine-structure [5] predictions.

By contrast, other atomic parameters such as transition rates are much harder to determine—both experimentally and theoretically—with accuracies often at the percent level. The behavior of the transition rates of heliumlike atoms in an isoelectronic sequence is a case in point that has received considerable theoretical attention [6]. A number of experimental determinations of the transition rates of highly ionized heliumlike species have tested these QED predictions, but there have been no published measurements of the decay of helium atoms from the 2^3P states to the ground state. This Letter presents the first measurement of the helium $2^3P_1-1^1S_0$ transition rate, providing a benchmark for other isoelectronic measurements in this sequence.

Helium has a simple electronic structure consisting of singlet (spin antiparallel) and triplet (spin parallel) excited states, of which the triplet manifold is connected by weak transitions that would otherwise be spin-forbidden to the 1^1S_0 (singlet) ground state (Fig. 1). The first excited state

(2^3S_1 , some 20 eV above the ground state) is distinguished by the fact that it is also forbidden by parity selection rules from decaying via an electric-dipole transition to the ground state and, consequently, has a very long (metastable) lifetime of $\tau \sim 8000 \text{ s}$ [7], to our knowledge the longest of any atomic species yet measured. Thus metastable 2^3S_1 helium can effectively be employed as a “ground-state” species for many atom optics and Bose-Einstein condensation experiments [8]. Excitation to the 2^3P states is readily achieved using 1083 nm laser radiation, which is used to laser cool and trap metastable helium atoms via the $2^3S_1-2^3P_2$ transition.

Transition rates from the 2^3P manifold are dominated by rapid decay back to the 2^3S_1 metastable level (inverse

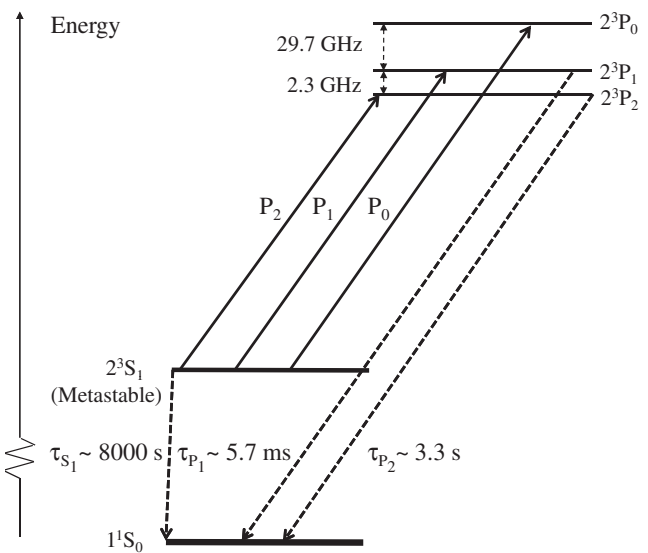


FIG. 1. Energy level diagram for helium showing the inverse decay rates (τ) for the helium $n = 2$ triplet manifold to the ground state.

decay rate $\tau \sim 98$ ns). However, apart from the 2^3P_0 level, which is strictly forbidden to decay by a single photon transition to the true ground state to all orders in the multipolar expansion, the 2^3P_1 and 2^3P_2 states have a small (but finite) probability of decay directly to the 1^1S_0 ground state via electric-dipole ($E1$) and magnetic-quadrupole ($M2$) transitions, respectively. Considerable theoretical work has been carried out to estimate these transition probabilities, with the first studies undertaken by Elton [9], who calculated the spin-orbit mixing of the 2^3P_1 state with the 2^1P_1 state to provide the principal decay contribution to the ground state. A more complete calculation including virtual transitions via other intermediate states was performed by Drake and Dalgarno [10], which was further refined by Drake [11]. Independent calculations using relativistic many-body perturbation theory performed by Johnson *et al.* [6] yielded similar results. Further refinement by Derevianko *et al.* [12] included the contribution due to negative-energy states, which, for helium, is very small. A rigorous derivation of the matrix elements for forbidden transitions in helium within QED theory, including relativistic corrections, was carried out more recently by Lach and Pachucki [13], providing further corroboration of the earlier calculations. Figure 2(a) summarizes the progress of these theoretical predictions for the 2^3P_1 decay rate to the helium ground state (including the result of the present experimental studies).

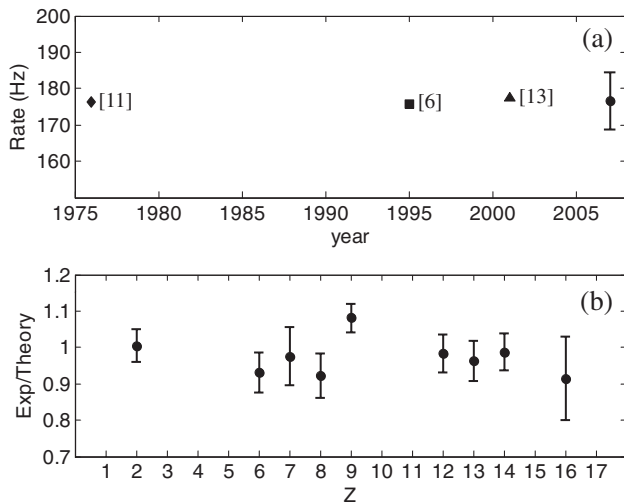


FIG. 2. (a) Historical progress of theoretical determinations for the helium $2^3P_1-1^1S_0$ decay rate (references shown), together with the experimental value (and uncertainty) from the present work. (b) Ratio of the experimental to the most recent theoretical decay rates, along with experimental uncertainties, for the $2^3P_1-1^1S_0$ transition in the heliumlike isoelectronic sequence. References (experimental, theoretical): He $Z = 2$, present work, [13]; C $Z = 6$ and N $Z = 7$ [14,15]; O $Z = 8$ [15,16]; F $Z = 9$ [6,16]; Mg $Z = 12$ and Al $Z = 13$ [6,17]; Si $Z = 14$ [15,18]; S $Z = 16$ [6,18].

However, measurement of the helium $2^3P_1-1^1S_0$ decay rate has proven much more elusive. This is in part due to the low transition probability which decreases rapidly lower down the helium isoelectronic sequence. Figure 2(b) shows the current state of experimental knowledge for this sequence relative to the most recent theoretical calculations. A further difficulty is that the predicted helium $2^3P_1-1^1S_0$ inverse decay rate of ~ 6 ms is many orders of magnitude larger than for the $2^3P_1-2^3S_1$ transition (~ 98 ns), which places severe requirements on the efficient measurement of signal levels given the typically low population of triplet-state helium atoms in conventional discharge sources [8]. In an early attempt (presented only in a conference abstract), Tang and Happer [19] used a helium discharge in which the fluorescence ratio between the $2^3P_1-1^1S_0$ and the $2^3P_1-2^3S_1$ transitions led to a $2^3P_1-1^1S_0$ decay rate of between 30 and 180 s^{-1} .

The more recent use of laser cooling and trapping techniques has enabled metastable helium atoms to be confined in a less perturbed environment more conducive to precision measurements. Nevertheless, accurate determination of transition rates has proven difficult even in a magneto-optic trap (MOT), due to a range of experimental difficulties in accurately determining the MOT conditions, and in ensuring a completely unperturbed environment [20]. Consequently, there has yet to be a published measurement of the $2^3P_1-1^1S_0$ transition rate in the open literature.

The present experiment aims to overcome these difficulties through a combination of techniques. First, the experiment is conducted in a UHV chamber ($< 10^{-11}$ mbar) designed for metastable helium Bose-Einstein condensation (BEC) experiments [21], which guarantees a long trap lifetime that enables measurement times extending to ~ 1 minute. Second, the measurement of the $2^3P_1-1^1S_0$ decay is performed in a relatively unperturbed environment by releasing the atoms momentarily from the trap. This is achieved by turning off the $2^3S_1-2^3P_2$ trapping laser (P_2 light) and briefly irradiating the slowly expanding cloud with a laser tuned near the $2^3S_1-2^3P_1$ transition (P_1 light). The presence of the P_1 light continually replenishes the 2^3P_1 population from the 2^3S_1 state, thereby ensuring that the $2^3P_1-1^1S_0$ decay rate dominates the decay rate due to the otherwise much faster $2^3P_1-2^3S_1$ transition.

To minimize any disturbance to the ultracold cloud by the P_1 laser beams, we take a number of precautions. First, we minimize the mechanical imbalance of the P_1 light by illuminating the trap with two equal counterpropagating laser beams tuned approximately $\delta_{\text{pop}} = 12\Gamma$ to the red of the P_1 transition (the trapping light is tuned $\delta_{\text{MOT}} = 20\Gamma$ to the red of the P_2 transition, where $\Gamma/2\pi = 1.6$ MHz is the natural linewidth). Second, the P_1 laser beams are aligned along one pair of MOT beams and polarized in the usual $\sigma^+ - \sigma^-$ trapping configuration. This ensures that any displacement due to imbalance in the P_1 beams can be compensated along the same axis by the P_2 beams

when the MOT is switched on again. Third, the power balance and alignment of the P_1 beams are adjusted such that they cause minimal perturbation to the MOT spatial profile. Finally, the detuning and intensity for the P_1 beams are chosen such that the P_1 population does not exceed the P_2 population ($\sim 6\%$). This ensures that the P_2 trapping light dominates the dynamics of the MOT.

The measurement process combines two key parameters: a determination of the P_1 population and measurement of the P_1 -induced trap loss. The P_1 population is determined using a saturated-fluorescence method similar to that we described previously [21]. Once the MOT is loaded to its steady-state value, the trap light is extinguished for a period of 200 μs , during which the P_1 excitation laser beams are turned on with a detuning of δ_{pop} and an intensity of I_{pop} . During this period, the fluorescence signal level F_1 (which was independent of the MOT magnetic field) is directly proportional to the number of atoms in the P_1 excited state. Immediately after this P_1 interrogation interval, the MOT light is turned back on for a period of 600 μs and the P_1 light is turned off, ensuring that all the atoms are recaptured into the MOT. Finally, a high intensity (approximately 2000 times the saturation intensity) pulse tuned to the P_1 resonance is used to produce a saturated-fluorescence signal F_{sat} while the P_2 light is again switched off. Since the same photodiode is used throughout the measurement, the P_1 population fraction during the interrogation period is simply given by $P_{1\text{pop}} = 0.5(F_1/F_{\text{sat}})$. Saturation is confirmed by increasing the power of the P_1 laser beams during the second pulse until no further increase in fluorescence is measured. A high speed InGaAs photodetector with a 50 μs rise time is employed, which is sufficiently fast to detect the peak of the saturated-fluorescence signal. After a short (10 ms) delay the sequence is repeated, but with no atoms loaded into the chamber in order to provide background signal subtraction.

The MOT is then reloaded, in order to determine the decay rate using a different diagnostic process. To measure the P_1 -induced trap loss, we monitor ion production from the MOT using a channeltron. The ion signal from the MOT is described by the following relation [22]:

$$\phi = \alpha N(t) + \frac{\beta}{4\sqrt{2}V} N(t)^2, \quad (1)$$

where β is the two-body Penning ionization rate constant, N is the number of trapped atoms, V is the volume of the MOT, and α is the one-body loss rate. To simplify the interpretation, all our experiments are performed in the one-body regime. This is achieved by first loading the MOT using an enhanced low-velocity intense source (LVIS⁺) beam [23] to reach a steady-state atom number. The LVIS⁺ beam is then switched off, and the MOT is allowed to decay via the various loss mechanisms. Initially, MOT loss is dominated by Penning ionization, but after

approximately 16 s the density has decayed sufficiently to allow this two-body term ($\propto N^2$) to be neglected (i.e., $\beta = 0$), leaving only the one-body background decay rate. At this point, the P_1 laser beams are turned on, with the same detuning δ_{pop} and an intensity I_{pop} as used in the population interrogation cycle. To avoid the added complication of having atoms in both the P_1 and P_2 excited states, which would ultimately lead to a slight correction to the P_1 population, we apply the P_1 laser beams in the absence of the P_2 trapping light, using a pulsed sequence. For 40 μs the trapping light is turned off, and the P_1 laser beams are turned on. The P_1 laser beams are then turned off and the trapping light is turned back on for 160 μs . This cycle is repeated until the number of atoms in the MOT has decayed to zero.

Without the P_1 light, this scheme does not cause additional trap loss since the trapped atoms move only a small distance relative to the size of the MOT beams during the 40 μs for which the trap is off. Also, since the atoms are only illuminated with the P_1 light for 20% of the time, any effect on the trapped atom cloud dynamics is reduced. Neither the duty cycle nor the length of the P_1 pulse has any effect on the measured decay rate, except for long ($>400 \mu\text{s}$) P_1 pulse durations when trap loss due to motional escape becomes apparent.

To obtain a P_1 decay time for a particular experimental run, the P_1 population is first measured during the P_1 interrogation pulse sequence. An exponential is then fitted to the following P_1 decay curve (see Fig. 3), after accounting for the one-body MOT decay time (~ 12 s—see the inset to Fig. 3) by dividing the measured P_1 decay curve by the background MOT decay curve.

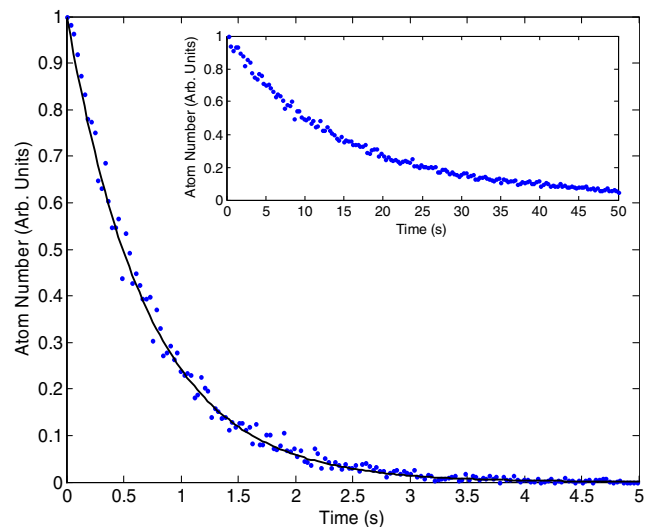


FIG. 3 (color online). Ion signal (data points with fitted exponential curve) recorded when the P_1 light illuminates the cloud of trapped atoms with a 20% duty cycle (P_1 population fraction 3.6%). The inset shows the case when the P_1 light is absent. $t = 0$ occurs ~ 16 s after the MOT loading is switched off.

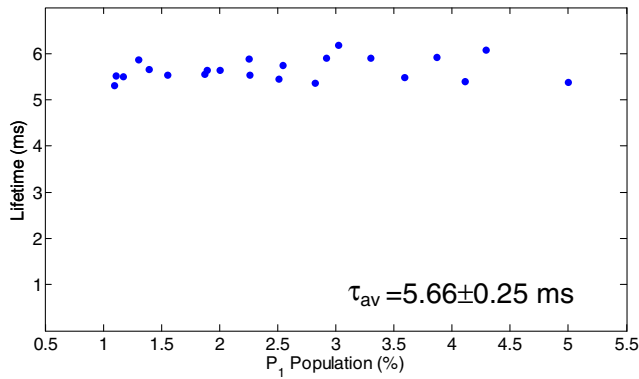


FIG. 4 (color online). Measured decay time versus P_1 population (each data point is an average over 10 decay curves).

The experiment is repeated for various δ_{pop} and I_{pop} which in turn yield different P_1 populations. A plot of P_1 decay time as a function of P_1 excitation percentage is shown in Fig. 4. Each data point represents the average over 10 decay curves, and the uncertainty in the exponential fit to the data (Fig. 3) is of the order of the size of the data points. Since any systematic variations arising from fluctuations in the laser frequency or intensity manifest themselves both in variations in the decay time and in the P_1 population, it is difficult to disaggregate the uncertainty in the ordinate and the abscissa in Fig. 4. It therefore is important to note that the decay time values show no systematic dependence on the P_1 population level (either due to changes in the laser intensity and/or detuning). The best indication of the uncertainty in the measurement is, therefore, the statistical spread in the data points, which is of the order of 4% (1σ). This is consistent with the observed variation ($<5\%$) in both the shot-to-shot MOT number and the laser intensity, and the averaging over 10 experimental decay curves.

Other possible sources of systematic error include motional effects from the laser beams, and the background atom loss. All experiments were performed in the regime where the $2^3P_1-1^1S_0$ decay rate dominated the trap lifetime, in which case background decay could be accounted for as outlined above. Furthermore, the experiments were conducted so that the P_2 beams dominated the MOT dynamics, and as indicated in Fig. 4, variation of the P_1 beam intensity or detuning had no effect (mechanical or otherwise) on the lifetime measurements.

The average value of the $2^3P_1-1^1S_0$ transition rate obtained over all measurements is $177 \pm 8 \text{ s}^{-1}$. This is in very good agreement with the theoretical calculations shown in Fig. 2(a) which themselves fall in a 1% band, the most recent value being 177.6 s^{-1} [13]. The value for the helium $2^3P_1-1^1S_0$ transition rate anchors the isoelec-

tronic sequence for this transition in Fig. 2(b) (the only value for $Z < 6$), and it also has a smaller uncertainty than the larger Z measurements. A similar situation [6] pertains to the $2^3P_2-1^1S_0$ transition for which there is no helium measurement, and for the $2^3S_1-1^1S_0$ transition where the only helium measurement has a very large uncertainty [7]. The determination of these transition rates is the subject of a future investigation in this laboratory.

We would like to acknowledge Chris Westbrook for helpful discussions and for providing a copy of the thesis by Julie Poupard. We also acknowledge Brenton Lewis and Peter Hannaford for careful reading of the manuscript. This work is supported by the Australian Research Council Centre of Excellence for Quantum-Atom Optics.

*kenneth.baldwin@anu.edu.au

- [1] D. C. Morton, Q. Wu, and G. W. F. Drake, *Can. J. Phys.* **84**, 83 (2006).
- [2] K. S. E. Eikema, W. Ubachs, W. Vassen, and W. Hogervorst, *Phys. Rev. A* **55**, 1866 (1997).
- [3] S. D. Bergeson *et al.*, *Phys. Rev. Lett.* **80**, 3475 (1998).
- [4] P. C. Pastor *et al.*, *Phys. Rev. Lett.* **92**, 023001 (2004).
- [5] G. Giusfredi *et al.*, *Can. J. Phys.* **83**, 301 (2005).
- [6] W. R. Johnson, D. R. Plante, and J. Sapirstein, *Adv. At. Mol. Opt. Phys.* **35**, 255 (1995).
- [7] H. W. Moos and J. R. Woodworth, *Phys. Rev. A* **12**, 2455 (1975).
- [8] K. G. H. Baldwin, *Contemp. Phys.* **46**, 105 (2005).
- [9] R. Elton, *Astrophys. J.* **148**, 573 (1967).
- [10] G. W. F. Drake and A. Dalgarno, *Astrophys. J.* **157**, 459 (1969).
- [11] G. W. F. Drake, *J. Phys. B* **9**, L169 (1976).
- [12] A. Derevianko, I. M. Savukov, W. R. Johnson, and D. R. Plante, *Phys. Rev. A* **58**, 4453 (1998).
- [13] G. Lach and K. Pachucki, *Phys. Rev. A* **64**, 042510 (2001).
- [14] R. Hutton, N. Reistad, L. Engström, and S. Hultdt, *Phys. Scr.* **31**, 506 (1985).
- [15] W. R. Johnson, I. M. Savukov, U. I. Safronova, and A. Dalgarno, *Astrophys. J. Suppl. Ser.* **141**, 543 (2002).
- [16] L. Engström *et al.*, *Phys. Scr.* **22**, 570 (1981).
- [17] I. A. Armour, J. D. Silver, and E. Träbert, *J. Phys. B* **14**, 3563 (1981).
- [18] S. L. Varghese, C. L. Cocke, and B. Curnutte, *Phys. Rev. A* **14**, 1729 (1976).
- [19] H. Y. S. Tang and W. Happer, *Bull. Am. Phys. Soc.* **17**, 476 (1972).
- [20] J. Poupard, Ph.D. thesis, Université de Paris-Sud, 2000.
- [21] R. G. Dall and A. G. Truscott, *Opt. Commun.* **270**, 255 (2007).
- [22] F. Bardou, O. Emile, J.-M. Courty, C. I. Westbrook, and A. Aspect, *Europhys. Lett.* **20**, 681 (1992).
- [23] J. A. Swansson, R. G. Dall, and A. G. Truscott, *Appl. Phys. B* **86**, 485 (2007).